NASA/TM—2003-212626

Jet Screech Noise Computation

Ching Y. Loh
Taitech, Inc., Beaver Creek, Ohio

Lennart S. Hultgren
Glenn Research Center, Cleveland, Ohio

October 2003

The NASA STI Program Office . . . in Profile

Since its founding, NASA has been dedicated to the advancement of aeronautics and space science. The NASA Scientific and Technical Information (STI) Program Office plays a key part in helping NASA maintain this important role.

The NASA STI Program Office is operated by Langley Research Center, the Lead Center for NASA's scientific and technical information. The NASA STI Program Office provides access to the NASA STI Database, the largest collection of aeronautical and space science STI in the world. The Program Office is also NASA's institutional mechanism for disseminating the results of its research and development activities. These results are published by NASA in the NASA STI Report Series, which includes the following report types:

- TECHNICAL PUBLICATION. Reports of completed research or a major significant phase of research that present the results of NASA programs and include extensive data or theoretical analysis. Includes compilations of significant scientific and technical data and information deemed to be of continuing reference value. NASA's counterpart of peer-reviewed formal professional papers but has less stringent limitations on manuscript length and extent of graphic presentations.

- TECHNICAL MEMORANDUM. Scientific and technical findings that are preliminary or of specialized interest, e.g., quick release reports, working papers, and bibliographies that contain minimal annotation. Does not contain extensive analysis.

- CONTRACTOR REPORT. Scientific and technical findings by NASA-sponsored contractors and grantees.

- CONFERENCE PUBLICATION. Collected papers from scientific and technical conferences, symposia, seminars, or other meetings sponsored or cosponsored by NASA.

- SPECIAL PUBLICATION. Scientific, technical, or historical information from NASA programs, projects, and missions, often concerned with subjects having substantial public interest.

- TECHNICAL TRANSLATION. English-language translations of foreign scientific and technical material pertinent to NASA's mission.

Specialized services that complement the STI Program Office's diverse offerings include creating custom thesauri, building customized databases, organizing and publishing research results . . . even providing videos.

For more information about the NASA STI Program Office, see the following:

- Access the NASA STI Program Home Page at ***http://www.sti.nasa.gov***

- E-mail your question via the Internet to help@sti.nasa.gov

- Fax your question to the NASA Access Help Desk at 301–621–0134

- Telephone the NASA Access Help Desk at 301–621–0390

- Write to:
  NASA Access Help Desk
  NASA Center for AeroSpace Information
  7121 Standard Drive
  Hanover, MD 21076

NASA/TM—2003-212626

Jet Screech Noise Computation

Ching Y. Loh
Taitech, Inc., Beaver Creek, Ohio

Lennart S. Hultgren
Glenn Research Center, Cleveland, Ohio

National Aeronautics and
Space Administration

Glenn Research Center

October 2003

Acknowledgments

The authors wish to thank Dr. J. Panda for fruitful discussions about the jet-screech phenomena, and for kindly providing his detailed experimental data. This work received support from the Supersonic Propulsion Technology Project Office of NASA Glenn Research Center.

The Propulsion and Power Program at
NASA Glenn Research Center sponsored this work.

Available from

NASA Center for Aerospace Information
7121 Standard Drive
Hanover, MD 21076

National Technical Information Service
5285 Port Royal Road
Springfield, VA 22100

Available electronically at http://gltrs.grc.nasa.gov

Jet Screech Noise Computation

Ching Y. Loh
Taitech Inc.
Cleveland, Ohio 44135
Email: c.y.loh@grc.nasa.gov

Lennart S. Hultgren
National Aeronautics and Space Administration
Glenn Research Center
Cleveland, Ohio 44135
Email: hultgren@nasa.gov

Abstract

The near-field screech-tone noise of a typical underexpanded circular jet issuing from a sonic nozzle is simulated numerically. The self-sustained feedback loop is automatically established in the simulation. The computed shock-cell structure, acoustic wave length, screech tone frequencies, and sound pressure levels in the near field are in good agreement with existing experimental results.

1 Introduction

Jet noise is an important and still challenging topic in aeroacoustics. Many of its aspects are of primary practical importance and the associated complicated physical phenomena are the topic of many experimental and theoretical investigations. References [1–4] provide a comprehensive discussion and further references. Under/over-expanded supersonic jets emit mixing noise, broadband shock-associated noise, as well as screech tones under certain conditions. The mixing noise is directly associated with large-scale structures, or instability waves, in the jet shear layer and the broadband shock-associated noise is caused by the interaction of these waves with the shock-cell structure in the jet core. The screech tones arise due to a feedback loop involving the large-scale structures developing in the jet shear layer, their interaction with the jet-core shock-cell structure producing upstream propagating acoustic waves, and re-generation of the large-scale structures at, or in the vicinity of, the nozzle lip. This feedback loop leading to screech tones is sensitive to small changes in the system conditions, and the understanding of the phenomena to date is based mostly on experimental observations [5–9]. Screech is of particular interest not only because of general noise-reduction concerns, but also because of potentially destructive structural interaction leading to sonic fatigue.

Reliable numerical simulation of jet screech noise, i.e., near-field noise computation in the presence of shock cells in the jet core, has only quite recently become feasible. It is a challenge in that the numerical scheme must: (i) handle shock waves, (ii) resolve acoustic waves with low dispersion and dissipation errors, (iii) resolve the instability waves in the jet shear layer and their interaction with the core shock-cell structure, and (iv) have an effective non-reflecting boundary condition. Successful direct computation of screech for circular jets have been carried out by Shen and Tam [10, 12] using the Dispersion Relation Preserving, or DRP, scheme and by the present authors [13–16] using a Navier-Stokes solver based on the space-time conservation element and solution element, or CE/SE, method [17, 18]. In their 3-D computation, Shen and Tam [12] adopted a spectral method in the azimuthal direction and by using only a limited number of spectral functions achieved substantial savings of computer memory and CPU time, without deterioration of accuracy. Other recent computational work includes [19, 20].

In general, the CE/SE method systematically solves a set of discretized space-time *integral* equations derived directly from the physical conservation laws and naturally captures shocks and other discontinuities in the flow. The

method may be categorized as a finite-volume method, where the conservation element (CE) is equivalent to a finite control volume (cell) and the solution element (SE) can be understood as the space-time cell interface. The scheme is second-order accurate in both space and time and the space-time surface fluxes are carefully calculated. Despite its formal second order accuracy, it possesses low dispersion error and low dissipation. Multi-dimensional non-reflecting boundary conditions (NRBCs), based on plane-wave propagation principles [21], are easily implemented. In principle, these NRBCs are equivalent to using characteristics but are simpler to apply. With these NRBCs, a small near field computational domain can be used. The CE/SE procedure is also easily adapted to complicated geometries using unstructured grids. The method is robust enough to cover a wide spectrum of compressible flow—from weak linear acoustic waves to shocks— hence, it is an appropriate tool for the present jet screech computation. Details of the method are described in [13, 17, 22].

2 The Axisymmetric Jet Screech Problem

Figure 1(a) shows the geometry of the convergent nozzle in Panda's experiment [9]. The flow is choked (i.e., Mach number $M_e = 1$) at the nozzle exit. The operating condition of the jet is fully described by additionally specifying the plenum (reservoir) to ambient pressure and temperature ratios, respectively. The pressure ratio is commonly expressed in terms of the jet Mach number, M_j, which would be the exit Mach number of the corresponding perfectly expanded jet. For the cold-flow situation (unity temperature ratio) considered in Ref. [9], the dominating screech tone mode is axisymmetric for $M_j \leqslant 1.19$. Hence, the numerical simulation can employ an axisymmetric CE/SE Navier-Stokes solver for these operational conditions. Furthermore, the attention is focussed here on the near field of the nozzle since this is the noise source region. The diameter, D, of the jet nozzle is chosen as the length scale; the density, ρ_∞,

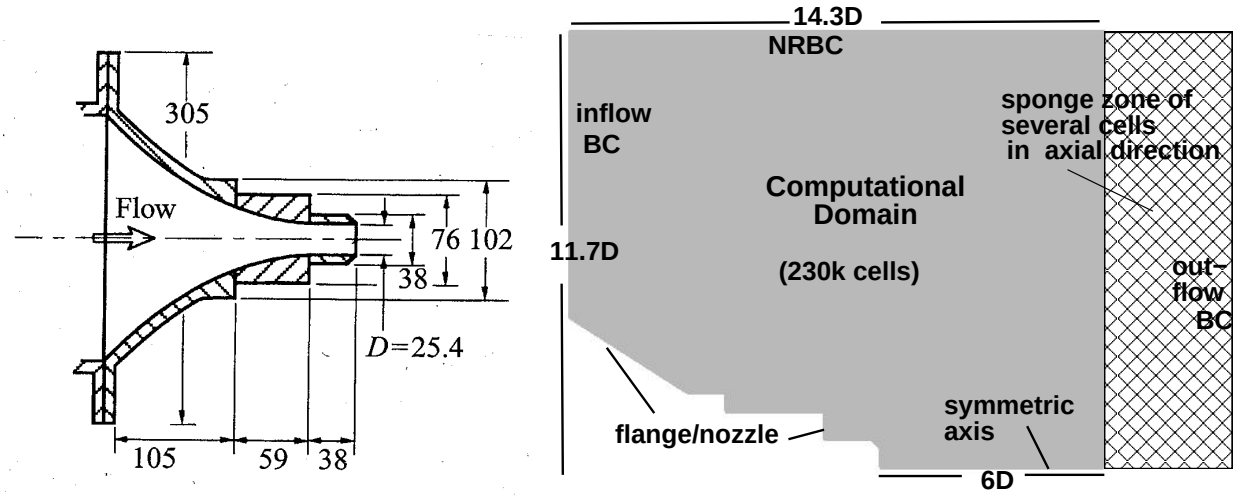

Figure 1. (a) Geometry of the convergent nozzle and flange in Panda's experiment [9] (dimensions in mm).
(b) Computational domain

speed of sound, a_∞, and temperature T_∞ in the ambient flow are taken as scales for the dependent variables; and all other scales are constructed from these. The computational domain, see Fig. 1(b), spans between $-8.3 \leqslant x \leqslant 6$ and $0 \leqslant r \leqslant 11.7$, with x and r being the nondimensional streamwise and radial coordinates. The flow inside the nozzle is not computed, rather the steady flow conditions are prescribed at the nozzle exit which is located at $x = 0$. This inflow plane is recessed by two cells so as not to numerically restrict or influence the feed-back loop. The numerical scheme [13, 14] utilizes a triangulated grid of about 230,000 cells. The triangular cells are generated by dividing rectangle-like quadrilaterals. Non-reflecting boundary conditions are applied to the upper and outflow boundaries and a symmetry condition is applied at the center axis. The last 10 streamwise cells are exponentially stretched and serve

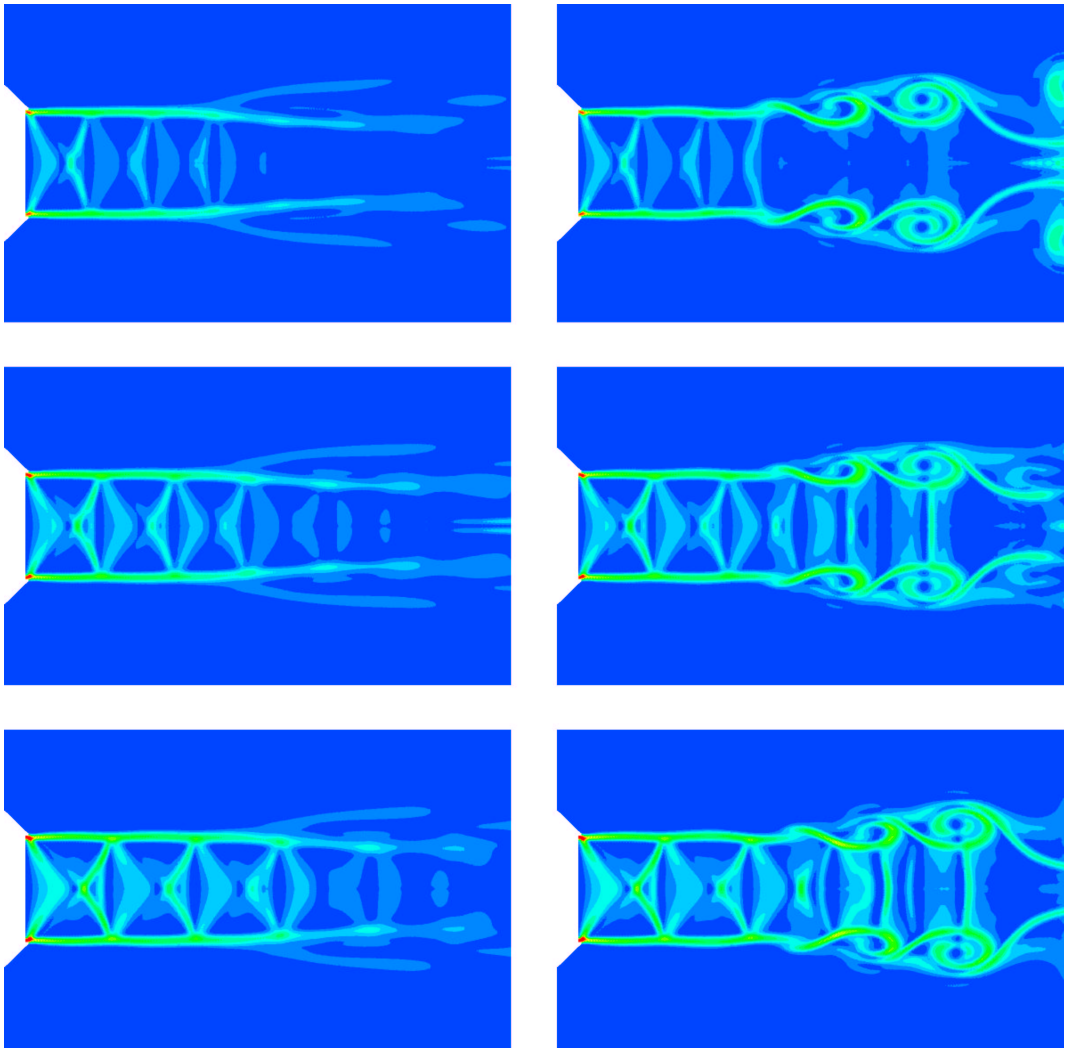

Figure 2. Numerical schlieren results (density gradient modulus) at $t = 410,000$ steps; $M_j = 1.11$, 1.15, and 1.19 in top, middle, and bottom rows; time-averaged and instantaneous results in left and right columns

as a buffer, or sponge, zone to essentially eliminate any small remaining numerical reflection from the downstream outflow boundary.

Initially, the entire flow field is at rest and at ambient conditions, *i.e.*, (using nondimensional variables)

$$\rho_0 = 1, \quad p_0 = \frac{1}{\gamma}, \quad T_0 = 1, \quad u_0 = 0, \quad v_0 = 0,$$

where ρ, p, T, u, v, and γ denotes the density, static pressure, temperature, streamwise velocity component, radial velocity component, and constant specific heat ratio, respectively. The jet flow is then impulsively started. At the inlet boundary, the conservative flow variables (see Appendix Eq. 2) and their spatial derivatives are specified to be those of the ambient flow, except at the nozzle exit, where an elevated pressure is imposed, *i.e.*, the jet is under-expanded, as in the physical experiments. By using the ideal gas isentropic relations, it follows that the nondimensional flow variables

Figure 3. Experimental schlieren picture showing the shock-cell structure for $M_j = 1.19$ [9, Fig. 5(b)]

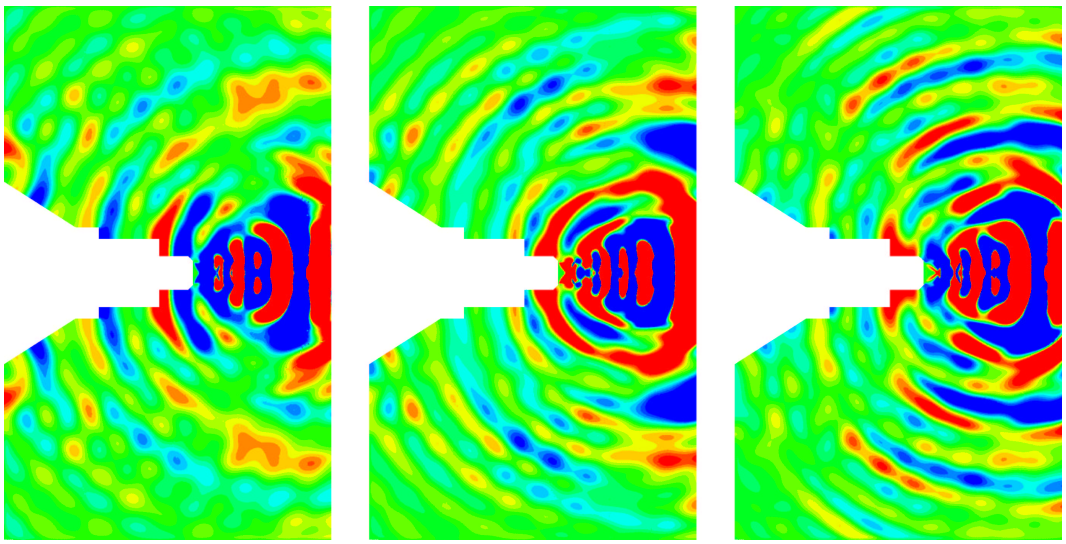

Figure 4. Instantaneous differential isobars, at t=410,000 steps, showing screech waves; $M_j = 1.11$, $1,15$, and 1.19 in left, middle, and right panels

at the nozzle exit, with $M_e = 1$, are given by

$$\rho_e = \frac{\gamma p_e}{T_e}, \qquad p_e = \frac{1}{\gamma}\left[\frac{2+(\gamma-1)M_j^2}{\gamma+1}\right]^{\frac{\gamma}{\gamma-1}}, \qquad T_e = \frac{2T_r}{\gamma+1}, \qquad u_e = T_e^{1/2}, \qquad v_e = 0,$$

where T_r is the reservoir (plenum) temperature. We will also follow the experimental cold-flow condition where the reservoir temperature equals the ambient one, *i.e.*, $T_r = 1$. The Reynolds number $Re = Da_\infty/\nu = 570,000$, where ν is the kinematic viscosity at the ambient conditions. The weighted average a-ϵ CE/SE scheme [22] is used with the weighting parameter $\alpha = 1$ and $\epsilon = 0.5$ in the present computation.

3 Numerical Results and Comparison to Experiments

In this section, various computed results are compared to the experimental findings of Panda [9]. Figure 2 displays numerical schlieren (density gradient modulus) contours, well after the start-up transients have passed out of the computational domain for the cases of $M_j = 1.11$, 1.15, and 1.19—top, middle, and bottom rows, respectively. The left and right columns show time-averaged and instantaneous results, respectively. The figure clearly displays the shock-cell structure as well as its deformation and destruction by the spatially growing large-scale structures in the

jet shear layer. The shock-cell spacing of $0.8D$ at $M_j = 1.19$ agrees well with the experimental result of Panda [9, Fig. 5(b)], reproduced here as Fig. 3.

Figure 4 displays instantaneous numerical isobars well after the start-up transients have passed out of the computational domain for the cases of $M_j = 1.11$, 1.15, and 1.19. The contours shown are for the fluctuating part of the pressure, i.e., the time-averaged pressure at each spatial location has been subtracted. Distinct screech waves are observed to emit from the 3rd to the 5th shock-cell and are reflected at the flange/nozzle body. The screech wavelength ($1.6D$) at $M_j = 1.19$ agrees well with the experiment [9]. Spectral analysis yields a computed screech frequency of 8513 Hz, which agrees well with the experimental value of 8525 Hz. Figure 5 displays computed sound pressure

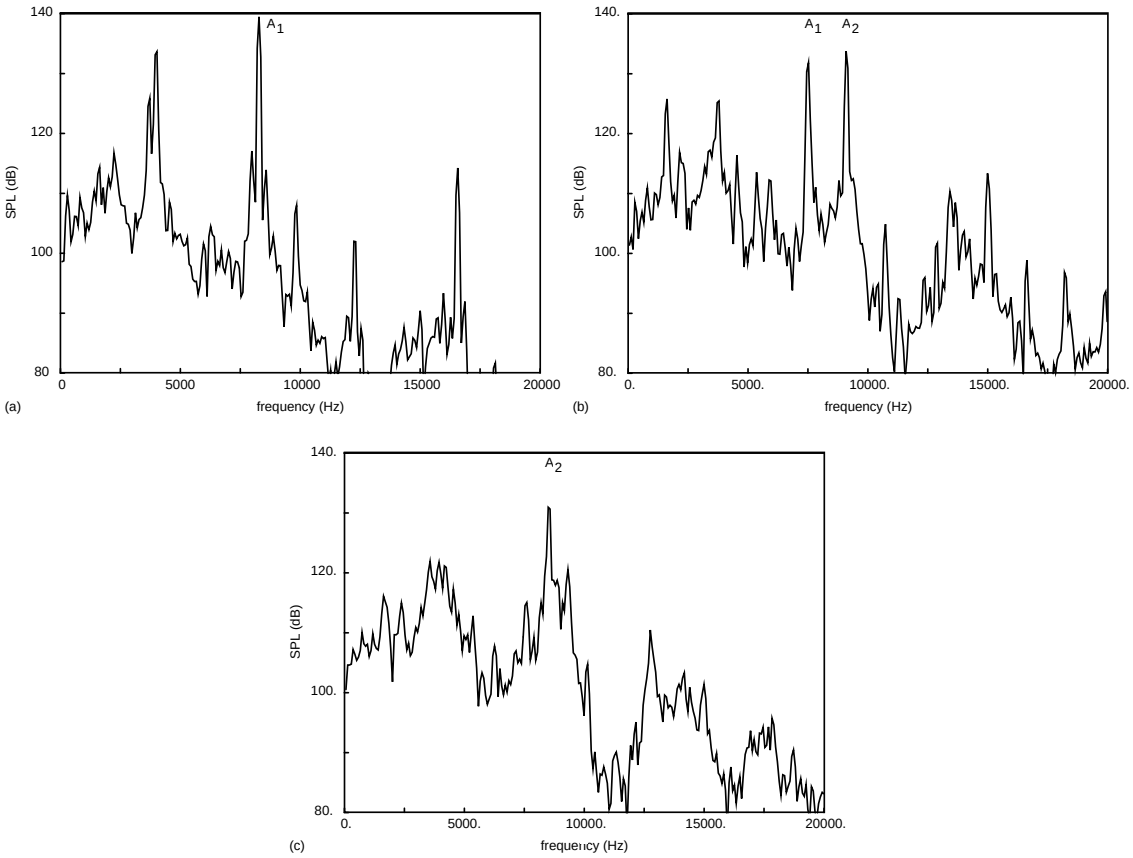

Figure 5. Narrow-band SPL distribution at nozzle exit ($x = 0$, $r = 0.6$), 75 Hz digital binwidth; (a) $M_j = 1.11$, A_1: 8289 Hz; (b) $M_j = 1.15$, A_1: 7542 Hz, A_2: 9110 Hz; (c) $M_j = 1.19$, A_2: 8513 Hz

level, SPL, distributions (narrow-band) at the nozzle exit lip wall ($x = 0$, $r = 0.6$) for $M_j = 1.11$, 1.15, and 1.19. The SPL distributions show distinct spikes corresponding to the A_1 and A_2 axisymmetric screech-tone modes observed in Panda's [9] experiment. For $M_j = 1.15$, both the A_1 and A_2 modes are dominating features, whereas only the A_1 mode is dominating at $M_j = 1.11$ and only the A_2 mode is dominating at $M_j = 1.19$. Note that in our earlier work [13], where a much simplified description of the nozzle external geometry was used, the A_1-mode screech tone (not observed in [9]) was also prominent at the latter jet Mach number. This illustrates the sensitivity of the screech phenomenon to geometry changes. Figure 6 shows a comparison of the current numerical with Panda's experimental results for the A_1 and A_2 screech-tone frequencies and SPL at the nozzle lip, both as functions of the jet Mach number. The screech-tone frequencies are well predicted, whereas the numerical SPL values are somewhat low.

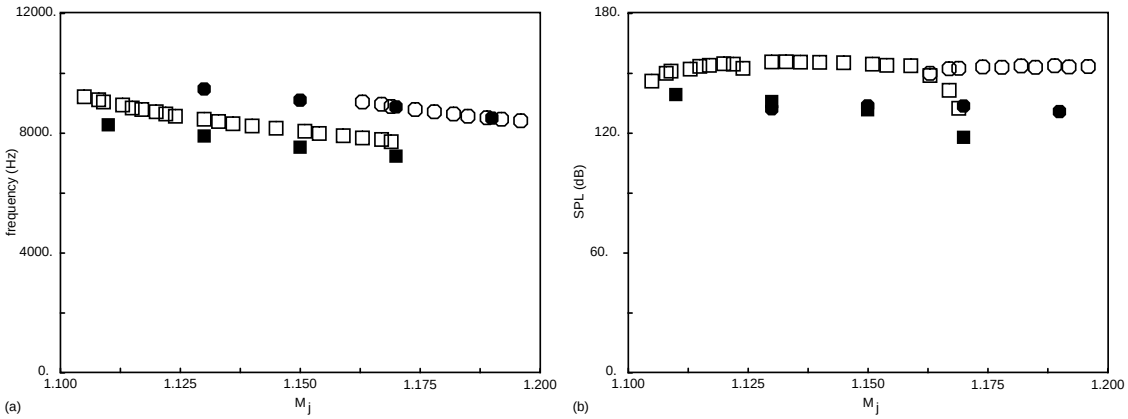

Figure 6. (a) Screech-tone frequency vs. M_j. (b) Screech-tone SPL at nozzle exit ($x = 0$, $r = 0.6$) vs. M_j. Square: A_1 mode, circle: A_2 mode; filled symbol: numerical simulation, open symbol: Panda's experiment

The SPL along an inclined line at the outer edge of the shear layer is shown in Fig. 7 for $M_j = 1.19$. This figure shows Panda's [9] data for the A_2 axisymmetric screech mode, the corresponding result from the simulation, as well as the computed total SPL and subharmonic of the A_2 mode. Even though the A_2 SPL level in the vicinity

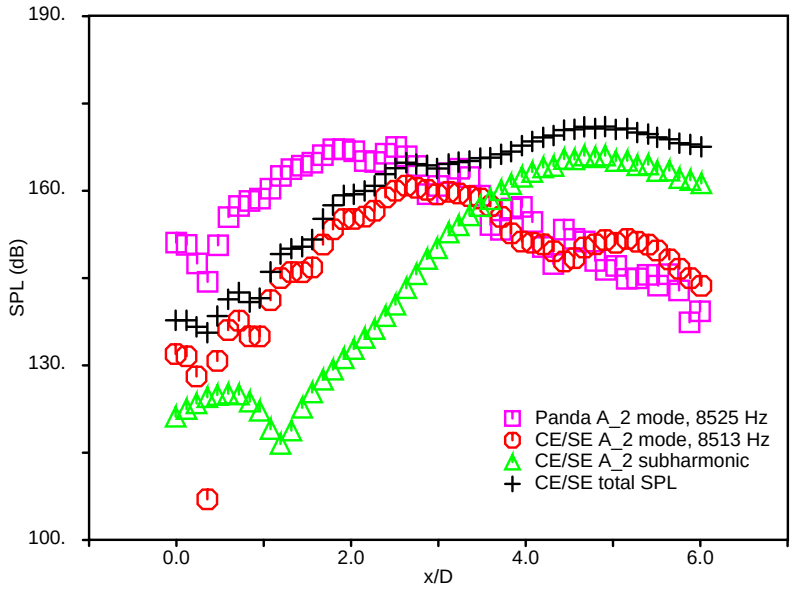

Figure 7. Comparison of computed and experimental [9] SPL along the shear layer edge, $M_j = 1.19$

of the nozzle lip is too low, its early streamwise growth rate is, however, well predicted indicating that the jet shear layer is in general well resolved. Nonlinearity in the shear layer limits the amplitude that can be obtained and once the SPL level 'catches up' the agreement is very good, in particular the SPL level in the streamwise region where the backward radiating acoustic waves are generated is well predicted. The strong subharmonic that appears further downstream is due to (axisymmetric) vortex pairing in the shear layer and as a consequence a second streamwise peak

at the A_2 frequency occurs due to nonlinear effects. However, 3-D effects are most likely to have come into play in the experiment at these streamwise locations leading to suppression of the subharmonic. The subgrid-scale eddy-viscosity model used in the present computation (see Appendix Eq. 3) does reduce the subharmonic somewhat, but cannot supress it since the model does not describe the effects of large-scale 3-D motions that ultimately become important at these streamwise locations. The reason for the low SPL values at the nozzle lip in the simulation is currently being pursued.

Figure 8 shows computed SPL contours for the A_2 mode. As in the experiment [9], a standing wave structure can be observed along the edge of the jet shear layer. As explained by Panda [9], the standing wave formation is due to combination of the downstream-propagating hydrodynamic and upstream-propagating acoustic fluctuations, both integral parts of the screech feedback loop. The results are in general agreement with the experimental ones except, as pointed out earlier, that the computed SPL levels are too low in the vicinity of the nozzle lip and the existence of a second, or extended, region of elevated values further downstream ($x/D > 4$).

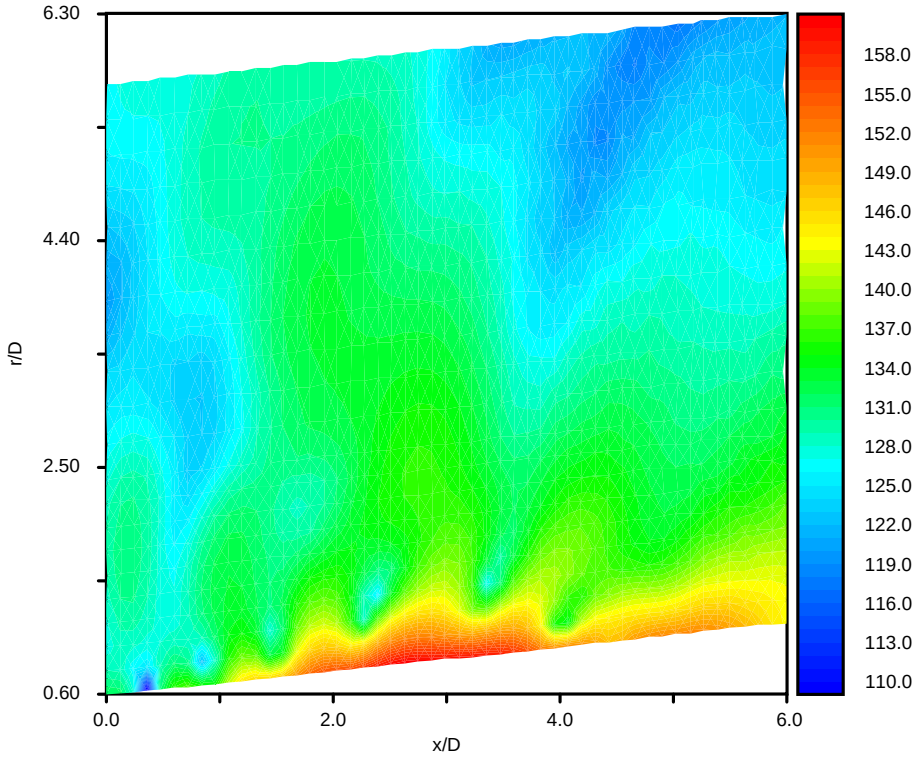

Figure 8. Computed A_2-mode SPL levels for Panda's experiment [9], $M_j = 1.19$

4 Concluding Remarks

In this paper, screech-tone noise analysis of an underexpanded supersonic axisymmetric jet was carried out using a finite-volume numerical scheme. Many hydrodynamic and acoustic aspects of the computed results are in good agreement with experimental findings [8, 9], including the variation of screech frequency with Mach number for the axisymmetric A_1 and A_2 modes. Since no forcing was applied in these simulations, the numerical results clearly indicate the presence of a self-sustained oscillation. LES modeling was used to better capture the jet spreading further downstream, i.e., after the initial shear-layer roll up, but is not believed to be a critical element for the screech feedback loop. Note that screech is essentially an inviscid phenomenon. It is concluded that the simulation shows a reasonably

good agreement with experimental data in the streamwise region where the flow is expected to be predominantly axisymmetric and, hence, that jet screech is successfully simulated using the present scheme.

The advantages of the present scheme were confirmed in the simulation. The implementation did not require any special treatment or parameter selections to capture both the shock-cell structure nor the acoustics. The robust finite-volume NRBC in combination with buffer zones virtually eliminates numerical reflections and allows for an effective near-field computation. The use of an unstructured grid also offers flexibility for dealing with more complicated geometries.

Acknowledgements

The authors wish to thank Dr. J. Panda for fruitful discussions about the jet-screech phenomena, and for kindly providing his detailed experimental data. This work received support from the Supersonic Propulsion Technology Project Office of NASA Glenn Research Center.

Appendix: Governing Equations

The axisymmetric Navier-Stokes equations can be written in the following vector conservation form:

$$\boldsymbol{U}_t + \boldsymbol{F}_x + \boldsymbol{G}_r = \boldsymbol{Q}, \tag{1}$$

where x, $r \geqslant 0$, and t are the streamwise and radial coordinates and time, respectively. The four components of the conservative flow variable vector $\boldsymbol{U}$ are given by

$$U_1 = \rho, \quad U_2 = \rho u, \quad U_3 = \rho v, \quad U_4 = p/(\gamma-1) + \rho(u^2+v^2)/2. \tag{2}$$

The components of the flux vectors $\boldsymbol{F}$ and $\boldsymbol{G}$ are given by

$$F_1 = U_2, \quad F_2 = (\gamma-1)U_4 + \left[(3-\gamma)U_2^2 - (\gamma-1)U_3^2\right]/2U_1 - \mu(2u_x - \tfrac{2}{3}\Delta), \quad F_3 = U_2U_3/U_1 - \mu(u_r + v_x),$$

$$F_4 = \gamma U_2U_4/U_1 - (\gamma-1)U_2\left[U_2^2+U_3^2\right]/2U_1^2 - \mu\left[2uu_x + v(u_r+v_x) - \tfrac{2}{3}u\Delta + \frac{\gamma}{Pr}\frac{\partial}{\partial r}\left(\frac{U_4}{U_1} - \frac{u^2+v^2}{2}\right)\right],$$

$$G_1 = U_3, \quad G_2 = U_2U_3/U_1 - \mu(u_r + v_x), \quad G_3 = (\gamma-1)U_4 + \left[(3-\gamma)U_3^2 - (\gamma-1)U_2^2\right]/2U_1 - \mu(2v_r - \tfrac{2}{3}\Delta),$$

$$G_4 = \gamma U_3U_4/U_1 - (\gamma-1)U_3\left[U_2^2+U_3^2\right]/2U_1^2 - \mu\left[2vv_r + u(u_r+v_x) - \tfrac{2}{3}v\Delta + \frac{\gamma}{Pr}\frac{\partial}{\partial r}\left(\frac{U_4}{U_1} - \frac{u^2+v^2}{2}\right)\right],$$

where u_x, u_r, v_x, v_r are the spatial derivatives of the streamwise and radial velocity components, which can be written in terms of the conservative variables U_1, U_2, U_3 and U_4, with Pr $(= 0.72)$ being the Prandtl number, $\mu = 1/Re$ the nondimensional viscosity, and the velocity divergence

$$\Delta = u_x + v_r + v/r.$$

The four components of the 'source' term $\boldsymbol{Q}$ are given by

$$Q_1 = -U_3/r, \quad Q_2 = -U_2U_3/U_1r, \quad Q_3 = -U_3^2/U_1r, \quad Q_4 = -G_4(\mu = 0)/r.$$

The above nondimensional equations would form the basis for a direct numerical simulation (DNS). Currently, this is not fully feasible for the high Reynolds number flows of interest here. The present computations are of the large-eddy-simulation (LES) type [23], where scales smaller than the grid resolution are modeled. In this case, the equations above are considered the filtered ones governing the resolved scales, where ρ and p are to be interpreted as simply averaged over the subgrid scales and the other dependent variables are to be interpreted as Favré, *i.e.* density-weighted, averages. The simplest model for the effects of the unresolved scales on the motion is obtained by using a Boussinesq eddy-diffusivity assumption for the subgrid shear stresses and heat flux coupled by Smargorinsky's model for the eddy viscosity (eg. [24]), *i.e.*, μ above is replaced by

$$\mu = 1/Re + (C_s\delta)^2(S_{ij}S_{ij})^{1/2}, \tag{3}$$

where $S_{ij} = \frac{1}{2}\left(\frac{\partial u_i}{\partial x_j} + \frac{\partial u_j}{\partial x_i}\right)$ is the rate-of-deformation tensor, $\delta = (\delta x \delta r)^{1/2}$ is a local measure of the grid size, and C_s is a (nondimensional) constant. Note that the simplifying assumption that the subgrid-scale Prandtl number equals the laminar one is also made here—if it is not, then the G_4 component needs to be slightly modified.

Panda *et al.* [25] investigated the initial status of the shear layer at the nozzle exit using a molecular Rayleigh scattering technique for a range of Mach numbers that spans the current one of interest and found it to be nominally laminar. This means that the small-scale turbulence that needs to be modeled is mainly produced as the jet shear layer rolls up, hence it is limited to a certain region of the spatial computational domain. Consequently, in the present work, C_s is essentially set to zero for $r > 1.5$ or $x < 3$ and is linearly ramped up for $3 < x < 5$ to the value $C_s = 0.1$ (see [23]), which is then used for $r < 1.5$ and $x > 5$.

By considering (x, r, t) as coordinates of a three-dimensional Euclidean space, E_3, and using Gauss' divergence theorem, it follows that Eq. (1) is equivalent to the following integral conservation law:

$$\oint_{S(V)} \boldsymbol{H}_m \cdot \mathrm{d}\mathbf{S} = \int_V Q_m \mathrm{d}V, \qquad m = 1, 2, 3, 4, \tag{4}$$

where $S(V)$ denotes the surface around a volume V in E_3 and $\boldsymbol{H}_m = (F_m, G_m, U_m)$. These equations are discretized and solved using the $a-\epsilon$ weighted-average CE/SE scheme with $\alpha = 1$ and $\epsilon = 0.5$, see [13, 14, 22] for further details. Note that Fureby and Grinstein [26] have pointed out that applying flux limiters to finite-volume methods, even in the absence of any explicit LES assumptions, effectively leads to LES schemes with minimal implicit SGS models. They demonstrated through 'error' analysis of a particular scheme that the flux-limiters (essentially low-pass frequency filters) build into the algorithm produces additional terms in the equivalent differential forms of the momentum and energy equations that can be interpreted as the SGS stress tensor and flux, respectively. Hence, there is an additional implicit SGS model inherent in the particular CE/SE scheme used in addition to the explicit assumption in Eq. 3.

The computational domain was decomposed into 10 subdomains using the METIS mesh partitioning code [27] freely available from the University of Minnesota. The CE/SE solver implemented MPI [28], or message passing interface, calls to exchange pertinent data between neighboring subdomains. The parallel computations were carried out on the CW-7 Linux PC (PIII) cluster at NASA Glenn Research Center.

REFERENCES

[1] Seiner, J. M., "Advances in High Speed Jet Aeroacoustics," AIAA Paper 84-2275 (1984).

[2] Tam, C. K. W., "Jet Noise Generated by Large Scale Coherent Motion," NASA RP-1258, pp. 311-390 (1991).

[3] Tam, C. K .W., "Supersonic Jet Noise," Ann. Rev. Fluid Mech. vol. 27, pp. 17-43 (1995).

[4] Raman G., "Advancces in Understanding Supersonic Jet Screech: Review and Perspective," Prog. Aerosp. Sci. vol. 34, pp. 45-106 (1998).

[5] Ponton, M. K. and Seiner, J. M., "The Effects of Nozzle Exit Lip Thickness on Plume Resonance," *J. Sound Vib.*, vol. 154, pp. 531-549 (1992).

[6] Ponton, M. K., Seiner, J. M. and Brown, M. C., " Near Field Pressure Fluctuations in the Exit Plane of a Choked Axisymmetric Nozzle," NASA TM 113137 (1997).

[7] Panda, J., Raman, G. and Zaman, K. B. M. Q., "Underexpanded Screeching Jets from Circular, Rectangular and Elliptic Nozzles," AIAA paper 97-1623 (1997).

[8] Panda, J., "Shock Oscillation in Underexpanded Screeching Jets," *J. Fluid Mech.*, vol. 363, pp. 173-198 (1998).

[9] Panda, J., "An Experimental Investigation of Screech Noise Generation," *J. Fluid Mech.*, vol. 378, pp. 71-96 (1999).

[10] Shen, H. and Tam, C. K. W., "Numerical Simulation of the Generation of Axisymmetric Mode Jet Screech Tones," *AIAA J.*, vol. 36, pp. 1801-1807 (1998).

[11] Shen, H. and Tam, C. K. W., "Effects of Jet Temperature and Nozzle-Lip Thickness on Screech Tones," *AIAA J.*, vol. 38, pp. 762-767 (2000).

[12] Shen, H. and Tam, C. K. W., "Three-Dimensional Numerical Simulation of the Jet Screech Phenomenon," *AIAA J.*, vol. 40, pp. 33-41 (2002).

[13] Loh, C. Y., Hultgren, L. S., and Jorgenson, P. C. E., “Near Field Screech Noise Computation for an Underexpanded jet by the CE/SE Method,” AIAA Paper 2001-2252 (2001).
[14] Loh, C. Y. and Hultgren, L. S., “Computing Jet Screech - A Complex AeroacousticFeedback System”, presented at the 2nd Int’l Conference on CFD (ICCFD2), also NASA/TM-2002-211807 (2002).
[15] Jorgenson, P. C. E. and Loh, C. Y., “Computing Axisymmetric Jet Screech Tones Using Unstructured Grids,” AIAA Paper 2002-3889 (2002).
[16] Loh, C. Y, Himansu, A. and Hultgren, L. S., “A 3-D CE/SE Navier-Stokes Solver with Unstructured Hexahedral Grid for Computation of Nearfield Jet Screech Noise,” AIAA Paper 2003-3207, (2003).
[17] Chang, S.-C., Wang, X.-Y. and Chow, C.-Y., “The Space-Time Conservation Element and Solution Element Method—A New High Resolution and Genuinely Multidimensional Paradigm for Solving Conservation Laws,” J. Comp. Phys. vol. 159, pp. 89-136 (1999).
[18] Loh, C. Y., Hultgren, L. S. and Chang S.-C., “Computing Waves in Compressible Flow Using the Space-Time Conservation Element Solution Element Method,” *AIAA J.*, vol. 39, pp. 794-801 (2001).
[19] Imamoglu, B. and Balakumar, P. “Computation of Shock Induced Noise in Imperfectly Expanded Supersonic jets”, AIAA Paper 2002-2527 (2002).
[20] Al-Quadi, I. M. A. and Scott, J. N., “High-Order Three-Dimensional Numerical Simulation of a Supersonic Rectangular Jet,” AIAA Paper 2003-3238 (2003).
[21] Loh, C. Y, “On the Nonreflecting Boundary Condition for Hyperbolic Conservation Laws,” AIAA Paper 2003-3975, (2003).
[22] Wang, X.-Y. and Chang S.-C., “ A 2-D Non-splitting Unstructured Triangular Mesh Euler Solver Based on the Space-Time Conservation Element and Solution Element Method,” *C.F.D. J.* vol. 8, pp. 309-325 (1999).
[23] Lesieur, M. and Métais, O., “New Trends in Large-Eddy Simulation of Turbulence,” *Ann. Rev. Fluid Mech.*, vol. 28, pp. 45-82 (1996).
[24] Bogey, C., Bailly, C. and Juvé, D., “Noise Investigation of a High Subsonic, Moderate Reynolds Number Jet Using a Compressible Large Eddy Simulation,” *Theoret. Comput. Fluid Dyn.*, vol. 16, pp. 273-297 (2003).
[25] Panda, J., Zaman, K. B. M. Q. and Seasholtz, R. G., “Measurements of Initial Conditions at Nozzle Exit of High Speed Jets,” AIAA Paper 2001-2143 (2001).
[26] Fureby, C. and Grinstein, F. F., “Monotonically Integrated Large Eddy Simulation of Free Shear Flows,” *AIAA J.*, vol. 37, pp. 544-556 (1999).
[27] Karypis, G. and Kumar, V. “Multilevel k-way Partitioning Scheme for Irregular Graphs”, U. of Minnesota Dept. of Comp. Sc./Army HPC Research Center Tech. Report 95-064 (1995).
[28] website: http://www-unix.mcs.anl.gov/mpi

REPORT DOCUMENTATION PAGE

Form Approved
OMB No. 0704-0188

1. AGENCY USE ONLY (*Leave blank*)	2. REPORT DATE	3. REPORT TYPE AND DATES COVERED
	October 2003	Technical Memorandum

4. TITLE AND SUBTITLE

Jet Screech Noise Computation

5. FUNDING NUMBERS

WBS–22–708–90–25

6. AUTHOR(S)

Ching Y. Loh and Lennart S. Hultgren

7. PERFORMING ORGANIZATION NAME(S) AND ADDRESS(ES)

National Aeronautics and Space Administration
John H. Glenn Research Center at Lewis Field
Cleveland, Ohio 44135–3191

8. PERFORMING ORGANIZATION REPORT NUMBER

E–14184

9. SPONSORING/MONITORING AGENCY NAME(S) AND ADDRESS(ES)

National Aeronautics and Space Administration
Washington, DC 20546–0001

10. SPONSORING/MONITORING AGENCY REPORT NUMBER

NASA TM—2003-212626

11. SUPPLEMENTARY NOTES

Ching Y. Loh, Taitech, Inc., Beaver Creek, Ohio 45430; and Lennart S. Hultgren, NASA Glenn Research Center. Responsible person, Ching Y. Loh, organization code 5880, 216–433–3981.

12a. DISTRIBUTION/AVAILABILITY STATEMENT

Unclassified - Unlimited
Subject Categories: 01 and 64 Distribution: Nonstandard

Available electronically at http://gltrs.grc.nasa.gov

This publication is available from the NASA Center for AeroSpace Information, 301–621–0390.

12b. DISTRIBUTION CODE

13. ABSTRACT ***(Maximum 200 words)***

The near-field screech-tone noise of a typical underexpanded circular jet issuing from a sonic nozzle is simulated numerically. The self-sustained feedback loop is automatically established in the simulation. The computed shock-cell structure, acoustic wave length, screech tone frequencies, and sound pressure levels in the near field are in good agreement with existing experimental results.

14. SUBJECT TERMS

Jet screech noise; Computational aeroacoustics

15. NUMBER OF PAGES

16

16. PRICE CODE

17. SECURITY CLASSIFICATION OF REPORT	18. SECURITY CLASSIFICATION OF THIS PAGE	19. SECURITY CLASSIFICATION OF ABSTRACT	20. LIMITATION OF ABSTRACT
Unclassified	Unclassified	Unclassified	